Title: Comparative study of the regeneration characteristics of LiCl and a new mixed liquid desiccant solution

Author: Tao Wen, Lin Lu*(vivien.lu@polyu.edu.hk), Mai Li, Hong Zhong

Department of Building Services Engineering, the Hong Kong Polytechnic University, Hong Kong, China

Abstract: This study first fabricated a new mixed liquid desiccant solution via the addition of hydroxyethyl urea to traditional lithium chloride solution to reduce its causticity in a metal-based regenerator. The formula of the new solution—25% LiCl, 39% hydroxyethyl urea, and 36% water—was determined according to the vapor pressure measured with the static method. Accordingly, its basic thermal properties (e.g., vapor pressure, density, viscosity, and conductivity) were measured and compared with those of a 35% LiCl solution. The corrosion characteristics of the mixed solution and the LiCl solution were analyzed with an electrochemical testing method. The regeneration performances of the solutions were experimentally studied, and the results show that the new solution significantly reduced causticity due to the addition of hydroxyethyl urea and a reduction in the concentration of LiCl. The regeneration effectiveness showed an average relative increase of 14.1% because of the larger wetting ratio and greater fluctuation of falling film. The wetting ratio increased from 81.5% to 87.8%, and the standard deviation of the film thickness increased from 25.441 μm to 31.672 μm with more rigorous fluctuations. Finally, an empirical equation for regeneration effectiveness was developed with an average absolute relative deviation of 4.01%, which provides a useful guide for the design of regenerators.

Keywords: Lithium chloride, hydroxyethyl urea, mixed liquid desiccant, corrosion, falling film regeneration

Nomenclature			
d	Absolute humidity (g / kg)	λ	Thermal conductivity (W / $m.K$)
G	Flow rate (kg / s)	μ	Dynamic viscosity (Pa.s)
h	Enthalpy (kJ / kg)	ρ	Density (kg / m^3)
$LDCS$	Liquid desiccant cooling system	σ	Standard deviation
Δm	Regeneration rate (g/s)	Subscripts	
P	Vapor pressure (Pa)	a	Air
T	Temperature ($^{\circ}C$)	e	Equilibrium
X	Concentration (%)	in	Inlet
Greek symbols		out	Outlet
δ	Film thickness (μm)	s	Solution
η_{eff}	Regeneration effectiveness	w	Hot water

1 Introduction

A liquid desiccant cooling system (LDCS) deals separately with sensible and latent loads for the accurate control of both indoor temperature and humidity. In a LDCS, the sensible load of the processed air is handled with a cooling coil, and the latent load in terms of extra humidity is absorbed by a dehumidifier, which differs greatly from a conventional vapor compression system (VCS). In a traditional VCS, the processed air is cooled below the dew point to remove moisture. However, in many situations, the processed air must be reheated before it can be delivered into the air conditioning room, which is a waste of energy [1]. Compared with the VCS, which relies heavily upon electricity consumption, the LDCS can use waste heat and solar thermal energy during the process of regeneration [2]. According to a previous study, the energy saving potential of LDCS over VCS can reach 50% in certain working conditions [3]. Because it caters to the demands of energy conservation and emission reduction, LDCSs have drawn more and more attention over the past few decades [2, 4-8].

One subsystem of the LDCS is the liquid dehumidification system. As shown in Fig. 1, its function is to absorb water vapor from the processed air with a liquid desiccant with a relative low temperature and high concentration. After the absorption of water vapor, the strong solution must release water to maintain a balanced concentration for long-term stable operation. This process is carried out in the regenerator, as shown in Fig. 1. To achieve a positive mass transfer driving force

between the liquid desiccant and the ambient air, the solution should be heated to a relatively high level. Two strategies are adopted during this process: full heat exchange with the solution outflow from the regenerator in heat exchanger 1 and further heating by an external heat source in heat exchanger 2. Regenerator/dehumidifier can generally be classified into three categories: packed-bed dehumidifiers, falling film dehumidifiers, and indirect contact dehumidifiers [9]. Falling film dehumidifiers have many unique merits compared to the other two types, including easy manufacturing technology for internal heating and cooling to achieve greater efficiency, better wettability, and a lower likelihood of liquid carryover [10]. As a result, numerous studies adopted the falling film type of regenerator/dehumidifier in an LDCS system. The regenerator's configuration is very similar to that of a heat exchanger, which consists of primary and secondary solution flow channels. Several types of metals, including aluminum, copper, and stainless steel, are used in the manufacture of such components due to their good thermal properties, structural strength, and mature crafts during production. However, one serious problem with the use of metals in falling film regenerators is corrosion by the liquid desiccant. Obvious rusty spots corroded by the lithium chloride solution have been observed on aluminum, copper, and stainless steel 304 [9, 11]. On one hand, the serious erosion of liquid desiccant on metal greatly affects the component's reliability. On the other hand, it may influence the heat and mass transfer characteristics during regeneration as the surface of the falling film regenerator is changed. Solutions to prevent or mitigate corrosion include the development of new plate materials or new alternatives for the liquid desiccant. Some attempts by previous investigators are summarized and described as follows.

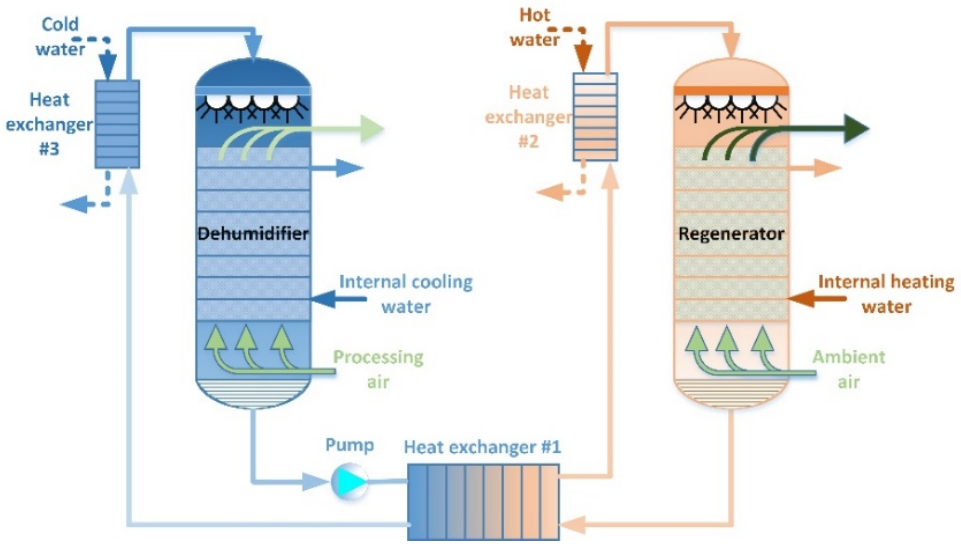

Fig. 1. Configuration of the liquid dehumidification subsystem.

In the aspect of manufacturing material, some studies have attempted to enhance the corrosion resistance performance of metal materials with the use of surface treatment technologies [9, 11]. Luo et al. [11] applied electroplating in the manufacture of a fin-tube dehumidifier. Electroplating was used to adhere certain kinds of anticorrosive materials to the dehumidifier surface to prevent corrosion from the liquid desiccant. An immersion corrosion test was used to prove the good anticorrosion performance of the electroplating dehumidifier. Wen et al. [9] conducted dehumidification experiments with an anodized aluminum plate regenerator. After surface treatment by anodizing, a dense aluminum oxide layer was paved on the surface of ordinary aluminum to avoid corrosion. Comparative corrosion and dehumidification tests were conducted, and the results indicated that an anodized plate dehumidifier not only greatly resisted corrosion from the salt liquid desiccant, but also improved the dehumidification performance. Other scholars have sought alternatives to metal-based dehumidifiers/regenerators [12, 13]. Lee et al. [13] used heat-resistant acrylonitrile butadiene styrene to produce a plastic-based dehumidifier. To overcome the plastic's poor wettability, a hydrophilic coating was applied to the dehumidifier's surface. Experiments were carried out to investigate the dehumidification performance, and correlations were developed to predict the heat and mass transfer coefficients. Liu et al.

[12] adopted another kind of plastic called thermally conductive plastic, with a thermal conductivity as high as 16.5 W/(m.K). Their experimental results demonstrated that the mass transfer performance of the plastic dehumidifier was comparable to that of a metal-based dehumidifier. However, the use of plastic for the manufacture of the regenerator/dehumidifier introduces several problems concerning wettability, manufacturing techniques, and structure strength that must be considered and solved before practical engineering application.

Salt solution liquid desiccants are the most common liquid desiccants, including lithium chloride (LiCl) solution, lithium bromide (LiBr) solution, and calcium chloride ($CaCl_2$) solution. Because $CaCl_2$ is likely to crystalize during application, the other two liquid desiccants are more prevalent in LDCSs. Unfortunately, they both seriously corrode the metal whether used alone or in combination [14]. In fact, in a previous study, a polyalcohol solution with no corrosion potential on metal was first used as the liquid desiccant [15]. For example, Elsarrag used triethylene glycol as the liquid desiccant and investigated its dehumidification performance in a packed-bed dehumidifier [15]. However, due to their low toxicity and volatility, the polyalcohol solution is not suitable for the application of dehumidification because the liquid desiccant directly contacts the processed air, which is distributed into the indoor environment and has a close relationship with the residents' health. As a compromise, some researchers used a mixture of salt solution and polyalcohol [16-18]. Tsai et al. [16] combined a lithium bromide/lithium chloride solution with triethylene glycol or propylene glycol to obtain a mixed liquid desiccant and measured their thermal properties. Similarly, they also combined a magnesium chloride solution with diethylene, triethylene, and tetraethylene glycol [17, 18]. Even though the mass transfer performance of the mixed solution developed by Tsai et al. [16-18] was preliminarily proven by the measurement results of vapor pressure, real experiments were not conducted to investigate the regeneration and dehumidification performance. In addition, the addition of polyalcohol to the salt solution liquid desiccant results in a health threat caused by the volatilization of polyalcohol. Luo et al. [19] regarded $LiNO_3$ as a promising candidate for the salt solution. Their experiments indicated that the $LiNO_3$ solution was less corrosive than

the LiBr solution for both carbon steel and stainless steel 304. They also measured the vapor pressure of the $LiNO_3$ solution at various concentrations and temperatures. Even though they investigated the performance for a refrigeration absorption system numerically with the $LiNO_3$ solution, experimental data were required to validate their simulation results. In addition to $LiNO_3$ solution, KCOOH solution is also regarded as a possible alternative to the conventional salt solution. Longo and Gasparella [20] studied its heat and mass transfer performance experimentally and numerically in a packed-bed dehumidifier. Another kind of mixed liquid desiccant was investigated by Donate et al. [21], who first measured the vapor pressure for a mixed solution with lithium bromide and organic salts of sodium and potassium. They then selected a proper combination for the mixed solution to study the water vapor absorption performance [22]. Their results suggested that the formula of LiBr+CHO_2Na+water (LiBr/ CHO_2Na=2 by mass) could be a promising candidate for the LiBr solution. However, their experiments were conducted in a vacuum for an absorption refrigeration system that was quite different from that of a dehumidification system.

Our literature review on liquid desiccants shows that even though some efforts have been made to replace the traditional salt liquid desiccant with a mixed solution, only the vapor pressure, which is the mass transfer driving force during regeneration, was studied, without further experimental study of the regeneration characteristics. As a result, our study first developed a new kind of mixed liquid desiccant by introducing hydroxyethyl urea into the LiCl solution to reduce its causticity. Unlike the mixed liquid desiccant introduced by previous researchers [16-18], it has no smell and is unlikely to become volatile outside the solution [23]. Hydroxyethyl urea has an excellent moisture retention capacity that is widely used in cosmetics [24]. Considering its mature application in other areas, its safety can be guaranteed. A formula for the mixed solution was determined according to the vapor pressure measured with the static method. For the first time, the corrosivity of a liquid desiccant was evaluated strictly by electrochemical methods. The corrosion behavior of stainless steel was studied and compared in both the mixed solution and the LiCl solution. Other thermal properties were measured, including density, viscosity, and thermal conductivity. To allow a direct

comparison of regeneration performance between the newly mixed liquid desiccant and the conventional LiCl solution, the regeneration performances of the mixed solution and the LiCl solution were identified and analyzed with a purpose-built experimental system. Finally, we developed a new theoretical correlation to predict the regeneration effectiveness to provide a useful guide for the design of regenerators.

2 Development of a new liquid desiccant based on vapor pressure

Hydroxyethyl urea was chosen for its lack of toxicity, lack of volatility, lack of odor, and excellent moisturizing capacity. To determine a suitable formula for the mixed solution, the 35% LiCl solution, which was appropriate for application in the LDCS, was selected for reference. A test bench (Fig. 2) was designed and constructed to measure the vapor pressure of the mixed solution. Fig. 2-a is a schematic diagram of the test system, and Fig. 2-b is a photograph of the experimental bench. The vapor pressure measurement is based on the static method [25], which means that when the mixed solution in the balance chamber achieves a balance with the vapor in the chamber at a certain temperature, the pressure of the vapor is the saturated pressure for the solution at that temperature. In the vapor pressure measurement system, the solution temperature was obtained with a Pt100 thermocouple with an accuracy of ±0.1 K. The vapor pressure was measured with an absolute pressure meter with an accuracy as high as 0.075%. System validation was conducted by measuring the saturation pressure of water at various temperatures before the formal experiments. Table 1 compares the measured vapor pressure and the reference data [26] for water. The mean absolute relative deviation (MARD) between the measured values and reference values is 0.99% when the vapor pressure varies from 2500 to 9200 Pa. It is thus reasonable to measure the vapor pressure of the mixed solution with the experimental system.

The most direct way to reduce the causticity of a liquid desiccant is to lower the concentration of LiCl and replace it with other kinds of desiccant. After many attempts, we found a nonvolatile, odorless, and nontoxic candidate: hydroxyethyl urea. However, a pure solution of hydroxyethyl urea has very limited dehumidification/regeneration capacity. As a result, it is necessary to add a certain amount of LiCl to the solution to enhance the dehumidification/regeneration capacity. In our study, 25% LiCl was added

to the mixed solution. The concentration of 25% LiCl is a compromise between the vapor pressure and the viscosity. During the experiments, it was found that the viscosity increased significantly as the hydroxyethyl urea concentration increased. On one hand, the high viscosity of the mixed liquid desiccant increases the power assumption of the pump in the system. On the other hand, it may lead to problems with hydrops and flow instability. It is also worth noting that the vapor pressure of the mixed liquid desiccant is lower at higher concentrations of LiCl, which benefits water vapor absorption. However, the higher concentration of LiCl corresponds to greater corrosivity. Finally, to maintain a balance between the vapor pressure and viscosity, the concentration of 25% was chosen for the mixed liquid desiccant, and 39% hydroxyethyl urea was then determined according to the vapor pressure. In fact, to obtain intuitive comparative results in terms of regeneration performance, we determined the concentration of hydroxyethyl urea according to the vapor pressure of 35% LiCl solution. That is to say, the hydroxyethyl urea was added gradually to the mixed solution until its vapor pressure was similar to that of 35% LiCl solution.

According to this method, the formula of the mixed solution is achieved with 25% LiCl + 39% hydroxyethyl urea +36% water. The vapor pressure of the new solution is shown in Fig. 3 at temperatures between 20°C and 60°C. With the addition of 39% hydroxyethyl urea into the 25% LiCl solution, the solution's vapor pressure is reduced significantly, as shown in Fig. 3. In addition, the vapor pressure of the mixed liquid desiccant shares nearly the same trend as 35% LiCl solution from 20°C to 50°C. Beyond 50°C, its vapor pressure is slightly lower than that of the 35% LiCl solution. The explanation is that the free energy of the solution is greater under a higher solution temperature, which increases the potential of water evaporation from the solution. Because the proportion of water in the 35% LiCl solution is higher than that in the mixed solution, its vapor pressure is naturally greater to achieve a balance at the surface of the solution. For convenience of application, the experimental data for the vapor pressure of the mixed solution were fitted to a polynomial equation with the solution temperature, as shown in Equation 1. The MARD between the measured values and the fitted ones is only 1.38%.

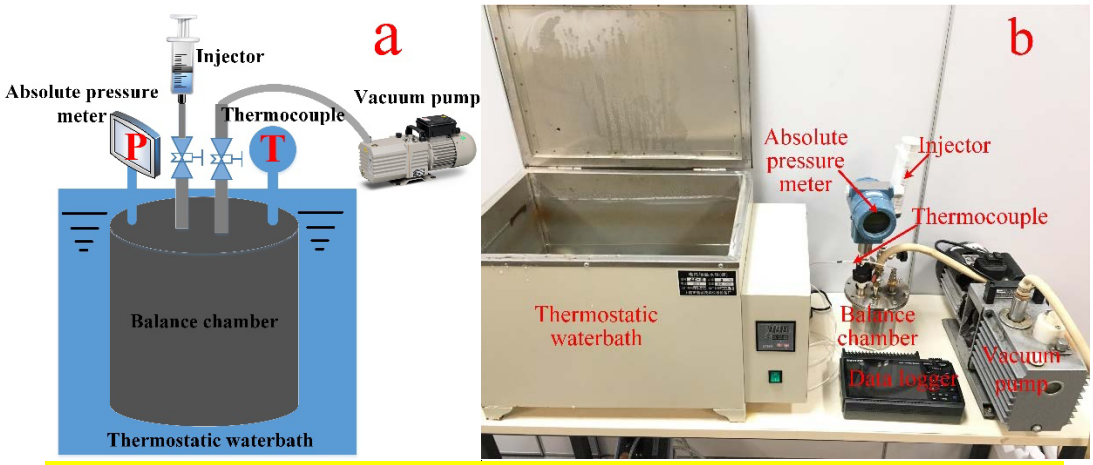

Fig. 2. Test bench for vapor pressure measurement: (a) schematic diagram; (b) real picture.

Table. 1. Comparison between measured and reference vapor pressure for water.

T/°C	21.5	24	28	30	33	35	37	38	42	44
Experiment	2521	2984	3745	4202	4985	5562	6143	6572	8175	9181
Reference	2566	2986	3783	4247	5035	5629	6282	6633	8210	9209
MARD/%	1.75	0.07	1.00	1.06	0.99	1.19	2.21	0.92	0.43	0.30

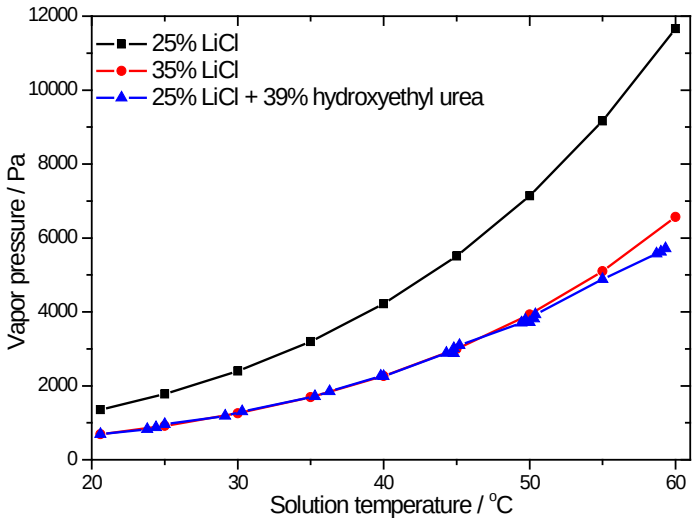

Fig. 3. Water vapor pressure of the new mixed liquid desiccant.

$$P_{sat} = -624.2118 + 113.2677T - 4.4309T^2 + 0.1109T^3 - 6.4138*10^{-4}T^4 \quad (1)$$

3 Corrosion behavior and thermal properties

3.1 Comparison of corrosion behavior

An electrochemical work station produced by Wuhan Corrtest Instruments Corp. [27] was used to identify the corrosion behavior. Because the regenerator investigated in this study was made of stainless steel, a sample was first prepared with the same

material. After polishing and cleaning with an ultrasonic cleaner, the surfaces of the stainless-steel sample were covered with nonconducting silicone rubber except for a 1.5 * 1.5-cm surface to provide exposure for electrochemical testing. During the test, the sample served as the working electrode. The calomel electrode and the platinum electrode were regarded as the reference electrode and the auxiliary electrode, respectively. The three electrodes connected to the work station were immersed in the tested solution. The Tafel polarization curves for both the 35% LiCl solution and the mixed solution were then obtained at the corresponding setting in the electrochemical work station. The scanning speed for the polarization curve was 1 mV/s, and the scanning range was −0.25V to 0.25V relative to the open circuit potential during the test [28]. Fig. 4 shows the Tafel polarization curves. Table 2 presents the corrosion behavior in terms of self-corrosion current and potential after the curves were postprocessed. According to the disciplines of corrosion [29], a greater self-corrosion current corresponds to a faster corrosion rate. For potential, the criterion is the reverse; that is, a greater potential corresponds to a slower corrosion rate. According to Table 2, the self-corrosion current of 0.2265 $\mu A/cm^2$ for the mixed solution is much lower than that of 6.799 $\mu A/cm^2$ for the 35% LiCl solution. The potential of the mixed solution is greater than that of the 35% LiCl solution. Moreover, the annual corrosion depth h_{corr} can be calculated by Equation (2) as follows [29]:

$$h_{corr} = 3.28\times10^{-3}\frac{M}{n\rho}I_{corr} \quad (2)$$

where M, n, and ρ are the molar mass, valence, and density of metal, respectively. I_{corr} is the self-corrosion current. According to Equation 2, the annual corrosion depth for the mixed solution and the LiCl solution are 0.08 mm/Y (mm per year) and 0.00267 mm/Y.

Therefore, based on the self-corrosion potential, the current, and the annual corrosion depth, the causticity of the newly developed mixed liquid desiccant on stainless steel 316L is much less than that of the 35% LiCl solution.

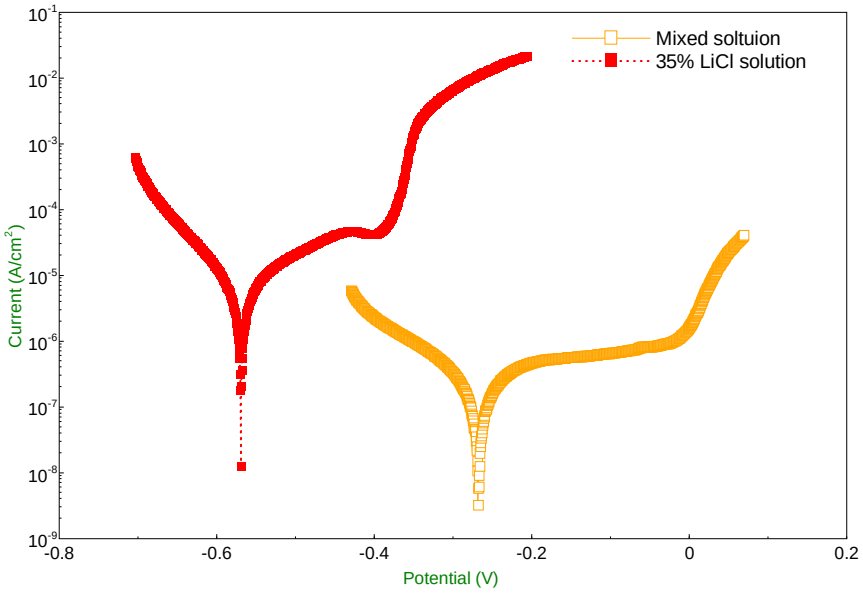

Fig. 4. Polarization curves for stainless steel in different solutions.

Table. 2. Comparison of corrosion characteristics in different solutions.

Solution	$E_{corr}(V)$	$I_{corr}(\mu A/cm^2)$	$h_{corr}(mm/Y)$
35% LiCl solution	-0.5683	6.799	0.08
New mixed solution	-0.2521	0.2265	0.00267

3.2 Density, viscosity, and thermal conductivity measurement

The thermal properties in terms of density, viscosity and thermal conductivity were measured and compared with those of 35% LiCl solution [30]. Table 3 lists the measuring instruments or sensors.

Table. 3. Specifications of the measuring instruments.

Property	Instrument	Accuracy
Density	Specific gravity hydrometer	$\pm 1 kg/m^3$
Viscosity	Rotational viscometer	±2%
Thermal conductivity	Thermal conductivity meter-TC3000E	±2%

Fig. 5 describes the results for density; it decreases gradually from 1258 kg/m^3 at 21.8°C to 1230 kg/m^3 at 60°C. At the same temperature, the density of the mixed solution is slightly greater than that of the 35% LiCl solution. However, such a tiny difference in density has negligible influence on heat and mass transfer performance during regeneration because density has no direct relationship with either heat or the

mass transfer driving force. A temperature-based polynomial was also developed for density, as shown by Equation 2. The MARD between the measured and predicted values is 0.02%.

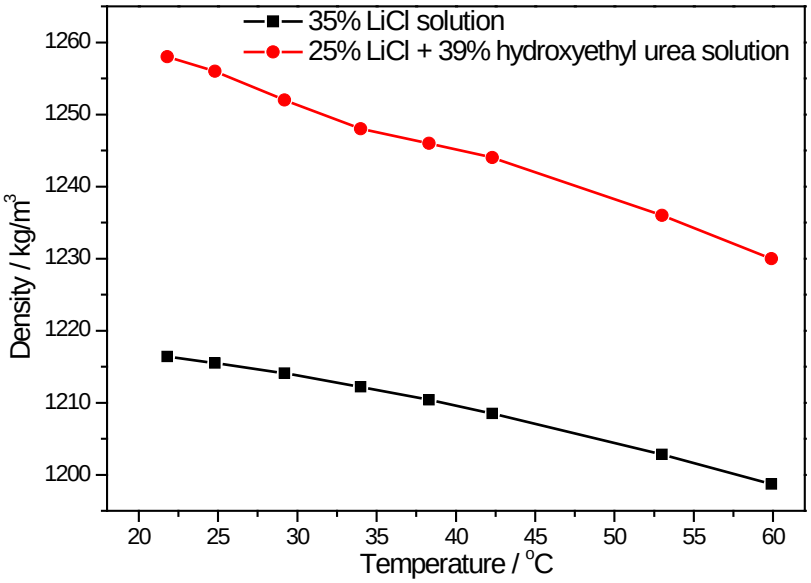

Fig. 5. Comparison of density between the mixed solution and the 35% LiCl solution.

$$\rho = 1295.5676 - 2.6515T + 0.0542T^2 - 5.2428 * 10^{-4}T^3 + 8.8861 * 10^{-7}T^4 \quad (2)$$

The dynamic viscosity of the mixed solution at various temperatures was measured with a rotational viscometer with an accuracy of ±2%. Fig. 6 compares the results with those of the 35% LiCl solution. The viscosity of the mixed solution is obviously much greater than that of the 35% LiCl solution. At 22°C, the viscosity of the mixed solution (15.24 mPa.s) is nearly three times greater than that of the 35% LiCl solution (5.65 mPa.s). As the solution temperature increases, the absolute difference between them decreases. From the point of view of viscosity, even though the addition of hydroxyethyl urea to the LiCl solution obviously reduces the concentration of LiCl and helps to maintain the mixed solution's low vapor pressure, the viscosity of the mixed solution is also significantly increased, which affects its flow characteristics in the system. On the one hand, according to Darcy's formula [31], the increase in the liquid viscosity increases the pressure drop of the fluid flow, which inevitably leads to greater power consumption by the pump in the system. On the other hand, the high viscosity

leads to hydrops in the solution duct, which correspond to the system's unsteady operation. Therefore, a balance exists between the mass friction of LiCl and hydroxyethyl urea in the mixed solution that will require more detailed investigation. Moreover, during the design of an LDCS with the new mixed liquid desiccant, a pump with greater input power will be required, and the ducts for the liquid desiccant must be well arranged to prevent accumulation of the liquid. A fitted correlation to describe the dynamic viscosity of the mixed solution at various temperatures is formulated by Equation 3, with a MARD of 0.56%.

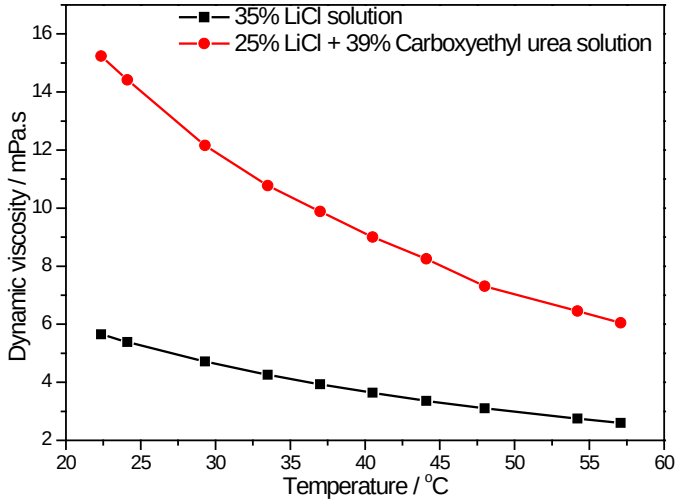

Fig. 6. Comparison of the dynamic viscosity of the mixed solution and the 35% LiCl solution.

$$\mu = 43.4204 - 2.3357T + 0.0674T^2 - 9.8806 * 10^{-4}T^3 + 5.6602 * 10^{-6}T^4 \quad (3)$$

A thermal conductivity Meter-TC3000E sensor was used to measure the thermal conductivities of the mixed solution at temperatures from 20°C to 60°C. Fig. 7 shows that the thermal conductivity of the mixed solution increases from 0.532 W/m.K at 21.2°C to 0.587 W/m.K at 60°C, which is slightly lower than that of the 35% LiCl solution at the same temperature. The lower thermal conductivity of the mixed liquid desiccant leads to slightly worse heat transfer performance between the liquid desiccant and the internal heating water. However, the thinness of the falling film makes such a performance difference negligible. A temperature-based polynomial is presented in Equation 4 to predict the thermal conductivity of the mixed solution. For all

experimental data, the mixed solution has a MARD of 0.23%.

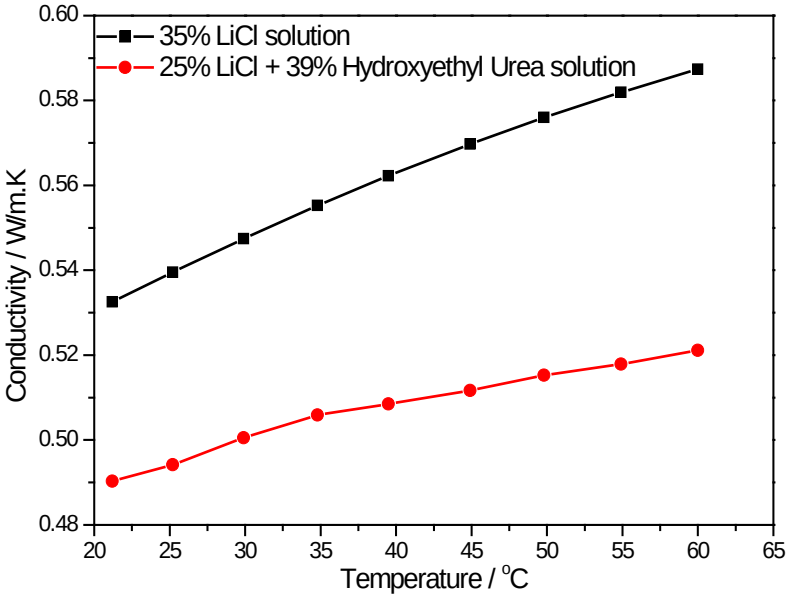

Fig. 7. Comparison of the thermal conductivity of the mixed solution and the 35% LiCl solution.

$$\lambda = 0.4678 + 3.0449 * 10^{-4} T + 6.4042 * 10^{-5} T^2 - 1.6231 * 10^{-6} T^3 + 1.1975 * 10^{-8} T^4 \quad (4)$$

4 Experimental method to determine regeneration performance

4.1 Description of experimental apparatus

Fig. 8 shows the experimental system used to investigate the regeneration performance of both the 35% LiCl solution and the new mixed solution. Three different working mediums—solution, air, and hot water—flow through three loops. In the solution loop, the solution stored in the tank is pumped into the plastic pipe. A cuboid plastic cavity with a narrow slit acts as the solution distributor. After the tank is filled with the solution, the solution spills over the distributor and flows along the plate regenerator. In this study, a 500 * 500-mm single-channel regenerator made of stainless steel 316L was used, as demonstrated in Fig. 9. After heat and mass transfer in the regenerator, the solution was collected and flowed to another tank. The temperature and flow rate of the solution were regulated with an automatic proportion-integration-differentiation controller and a three-way valve, respectively. For the air loop, an axial fan was used to direct ambient air into the air duct. To adjust the inlet air temperature

and humidity to set values, another automatic proportion-integration-differentiation controller and an electric humidifier were installed in the air duct, as shown in Fig. 8. The flow rate of air was controlled by a damper in the duct. When all setting parameters were satisfied, the air was distributed into the regenerator for regeneration. Hot water was added to improve the efficiency. During the regeneration process, due to the positive vapor pressure gradient between the solution and the air, water in the phase of liquid evaporated from the solution along with the absorption of the phase change latent heat. This leads to a reduction in the solution's temperature and a deterioration in the regeneration performance. The hot water circulates at the back of the solution and supplements heat for the solution to avoid a reduction in the solution temperature. The hot water was heated with an electric heater connected to an automatic controller and then pumped to the regenerator. After exchanging heat with the solution in the regenerator, the water flowed back to a water tank for the next circulation. Each of the loops mentioned above was covered by thermal isolation material neoprene foam to prevent heat exchange between the experimental system and the surrounding environment.

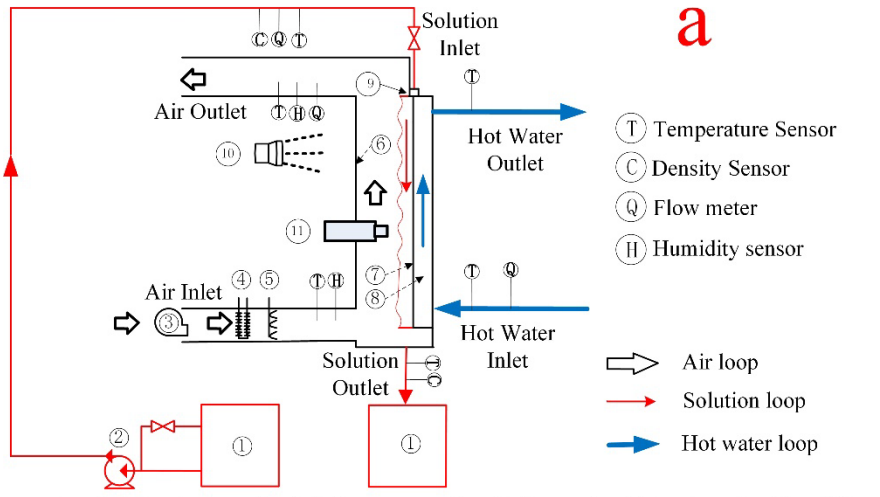

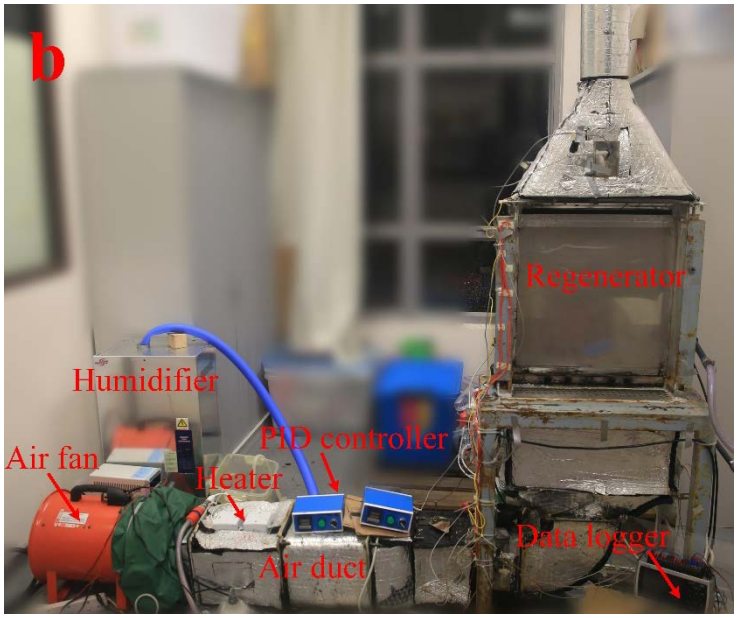

Fig. 8. Experimental system for regeneration: (a) schematic diagram; (b) real picture.

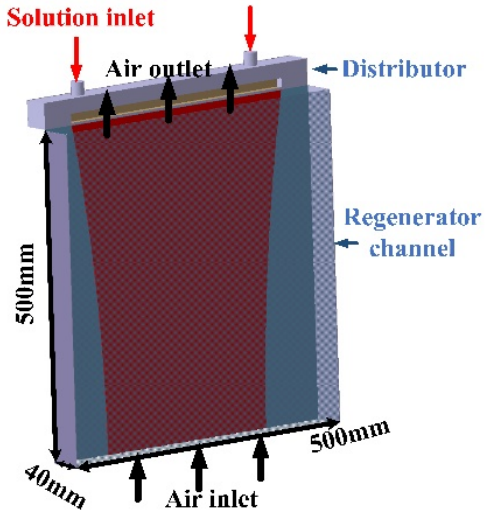

Fig. 9. Detailed information on the single-channel regenerator.

4.2 Data measurement and regeneration criteria

Two turbine flow rate meters with a relative accuracy of ±3% were used to measure the mass flow rates of the solution and the hot water. The flow rate of air was obtained by a pitot tube connected to a micromanometer; a measurement accuracy of 2.2% was obtained. Pt100 thermocouples with an accuracy of ±0.1K were used to measure all temperatures, including the air, the solution, the cooling water inlet, and the outlet temperature. Two humidity sensors installed before and after the regenerator were used

to measure the inlet and outlet relative humidity of the processed air. The absolute humidity content of the air was calculated from the dry bulb temperature obtained by the Pt100 thermocouple and the relative humidity.

In this study, we selected the regeneration rate and regeneration effectiveness as the performance indexes to evaluate the regeneration characteristics. The regeneration rate is defined as follows:

$$\Delta m = G_a (d_{a,out} - d_{a,in}) \qquad (5)$$

where G and d stand for the mass flow rate and the absolute humidity content, respectively. The subscript a indicates air, and the subscripts *in* and *out* distinguish the inlet and outlet parameters.

In fact, Equation 5 describes only the total humidity change in the air. However, according the law of mass conservation, the water that evaporates from the solution equals the increase in water vapor in air. Consequently, Equation 5 can also represent the amount of water regenerated from the solution, namely, the regeneration rate.

The regeneration effectiveness is defined and shown by the following equation:

$$\eta_{eff} = \frac{d_{a,out} - d_{a,in}}{d_e - d_{a,in}} \qquad (6)$$

in which d_e is the equivalent absolute moisture content of the solution in the condition of equilibrium at its inlet concentration and temperature. The regeneration effectiveness is the ratio between the absolute humidity change in the air and the greatest potential humidity change; it indicates the efficiency of the regenerator.

4.3 Uncertainty analysis

Uncertainty analysis for various study parameters was conducted according to the accuracy of the sensor and the uncertainty propagation method. Some parameters, such as the temperature, flow rate, and relative humidity, were measured directly with sensors. Therefore, their uncertainties were obtained based on the accuracies of the sensors. Other parameters, such as the absolute humidity content, the regeneration rate, and effectiveness, were calculated via conservation. As a result, their uncertainties were acquired by the uncertainty propagation method, as shown in Equation 7 [32]. Table 4 summarizes the results of the uncertainty analysis.

$$\frac{\delta y}{y}=\sqrt{(\frac{\partial \ln f}{\partial x_1}\delta x_1)^2+(\frac{\partial \ln f}{\partial x_2}\delta x_2)^2+...+(\frac{\partial \ln f}{\partial x_n}\delta x_n)^2} \quad (7)$$

Table. 4. Summary of the results of the uncertainty analysis.

Parameter	Uncertainty	Parameter	Uncertainty
Temperature/ T	± 0.1K	Hot water flow rate/ G_w	± 3%
Solution flow rate/ G_s	± 3%	Air absolute humidity/ d	2.7%
Air flow rate/ G_a	± 2.2%	Regeneration rate/ Δm	3.8%
Air relative humidity/ φ	± 2.5%	Regeneration effectiveness/ ξ	5.3%

4.4 Experimental validation

The uncertainty analysis of the parameters in the experimental study can only validate the reliability of a single parameter. To prove the rationality of the whole system, the energy and mass balance for the system were checked. The formulas for the conservation equations are shown by Equations (8) and (9).

$$G_s(h_{s,out}-h_{s,in})+G_a(h_{a,out}-h_{a,in})=G_w(h_{w,in}-h_{w,out}) \quad (8)$$

$$G_a(d_{a,in}-d_{a,out})=G_sX_{s,in}(\frac{1}{X_{s,out}}-\frac{1}{X_{s,in}}) \quad (9)$$

where the subscripts *s* and *w* stand for the solution and cooling water, respectively. h and X indicate the enthalpy and concentration of the solution.

In this study, the liquid concentration was obtained in an indirect manner. The solution's temperature and density were measured with a thermocouple (accuracy, 0.1K) and a specific gravity hydrometer (accuracy, 1 kg/m^3), respectively. The concentration was then obtained with the equation provided by Conde [30]. According to the measurement accuracies of the sensors and the uncertainty propagation method, the relative uncertainty for the concentration is no less than 0.195%. However, during the regeneration experiments, the relative change in the solution concentration was less than 0.195%, according to Equation (9). Therefore, it is unscientific and unreasonable to measure the outlet solution concentration due to the miniscule change during the experiments. It was also noted that during the process of regeneration, the heat and mass

transfer coupled together due to water vapor regeneration at the gas-liquid interface. From this point of view, the energy balance results may partially reflect the mass balance. Moreover, difficulty in mass balance validation was not found only in this study, but also in previous studies [33, 34]. Therefore, only the energy balance was checked with Equation 10. It is also worth noting that because the heat capacity of the newly developed solution was unknown, only the energy conservation equation for the 35% LiCl solution was checked. Fig. 10 shows the validation results. It can be concluded from the figure that nearly all of the enthalpy absolute differences between the right side and the left side of Equation 8 are less than 20%. The enthalpy differences are caused by the small amount of heat exchange between the experimental system and the ambient environment and the uncertainties in the measured parameters. The rationality of the experimental system can thus be validated by the energy balance results. Moreover, the uncertainties in the regeneration rate and the effectiveness under various operating conditions shown in the following section refer to the uncertainty analysis presented in Section 4.3.

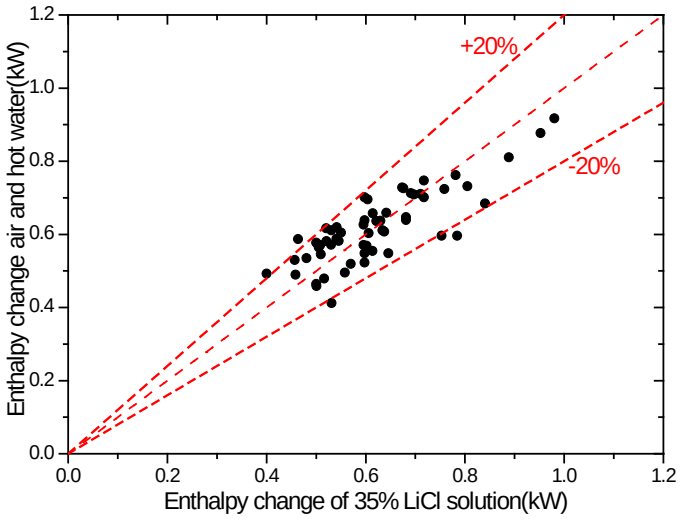

Fig. 10. Energy balance results for the experimental system.

5 Results for regeneration and discussion

5.1 Influence of air flow rate

Fig. 11 shows the influence of the air flow rate on the regeneration performance. When the air flow rate increases from 0.023 to 0.07 kg/s, the regeneration rate for the mixed solution also increases from 0.05 to 0.111 g/s. The same trend also applies to the

35% LiCl solution because of the increase in the mass transfer coefficient as the air velocity increases. The mass transfer coefficient increases from 0.0232 to 0.0540 kg/(m^2.s) for the 35% LiCl solution and from 0.0226 to 0.0547 kg/(m^2.s) for the mixed liquid desiccant. However, the opposite tendency is observed for the regeneration effectiveness. The effectiveness decreases from 17.9% to 14.5% for the mixed solution as the air flow rate increases. This reduction is caused mainly by the decrease in the contact time between the air and the liquid desiccant [9, 35]. During the regeneration process, when the air mass flow rate increased from 0.024 to 0.068 kg/s, the average air velocity in the regenerator increased from 0.57 to 1.62 m/s. As a result, the contact time was reduced from 0.88 to 0.31 s. A decrease in contact time leads to a reduction in the absolute humidity change, which is defined by the difference between the outlet and inlet absolute moisture contents. The absolute humidity change is also the numerator of the regeneration effectiveness, as shown in Equation 6, and its reduction results in a decrease in effectiveness because its denominator remains constant at various air flow rates. Clearly, both the regeneration rate and the effectiveness of the mixed liquid desiccant show a slight improvement compared with the 35% LiCl solution. The relative improvement ranges from 6.5% to 11.1% for the regeneration rate and from 4.5% to 9.2% for effectiveness.

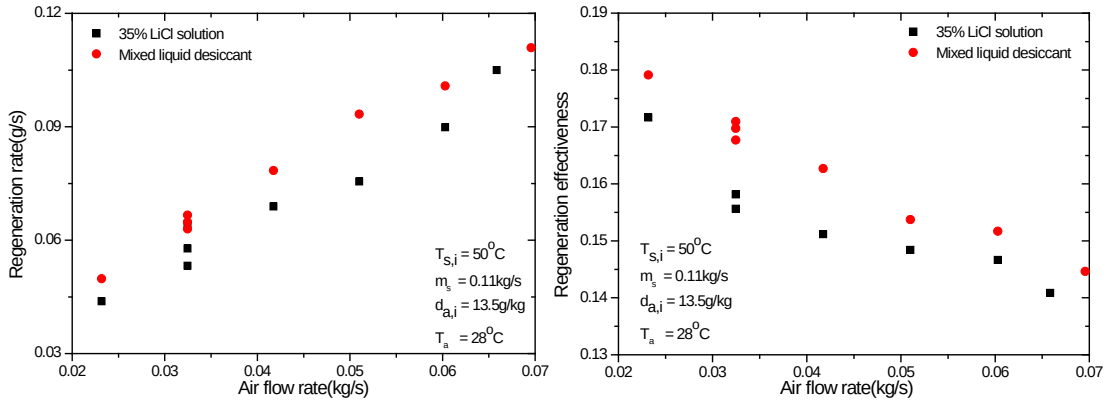

Fig. 11. Influence of air flow rate on regeneration.

5.2 Influence of air temperature

Fig. 12 shows the regeneration rate and effectiveness of both the mixed solution

and the 35% LiCl solution at air temperatures from 28°C to 36°C. It is obvious that both criteria remain almost unchanged at various air temperatures. The values for the regeneration rate fluctuate around 0.09 and 0.084 g/s for the mixed solution and for the 35% LiCl solution, respectively. The values for effectiveness are 15.9% and 13.1%. The ignorable influence of the air temperature can be attributed to its negligible effect on both the mass transfer driving force and the flow characteristics of the falling film. The mixed solution has a higher regeneration rate and greater effectiveness than the 35% LiCl solution, with average relative improvements of 6.4% and 19.3%, respectively. The 19.3% improvement in effectiveness is much greater than that in the regeneration rate (6.4%), which can be explained by the vapor pressure of these two liquid desiccants at 55°C in Fig. 3. At the regeneration temperature of 55°C, the vapor pressures of the mixed solution and the 35% LiCl solution are 4842 and 5099 Pa, respectively, which correspond to equivalent absolute humidity contents of 31.3 and 33.0 g/kg, respectively. According to the definition of effectiveness shown in Equation 6, the denominator is smaller for the mixed solution than for the 35% LiCl solution. Therefore, the relative improvement in effectiveness is greater than that in the regeneration rate.

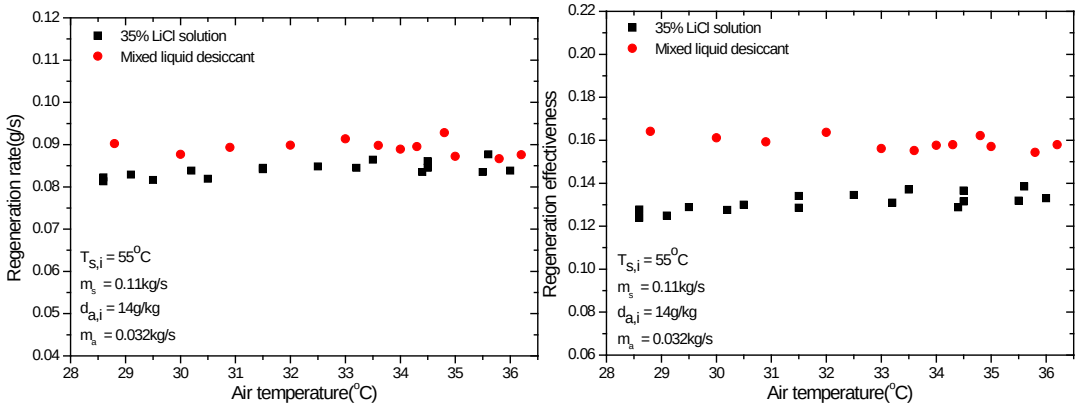

Fig. 12. Influence of air temperature on regeneration.

5.3 Influence of air humidity

Fig. 13 allows comparison of the regeneration performance at various levels of air humidity. When the air humidity gradually increases from 12.5 to 21.2 g/kg, the regeneration rate and effectiveness of the mixed solution decrease from 0.097 to 0.032

g/s and 15.7% to 10.0%, respectively. With the 35% LiCl solution, similar tendencies can be also observed in the regeneration rate and effectiveness. The declining trend is caused by the decrease in mass transfer in terms of the difference between the equivalent absolute humidity content of the solution and the air. Some interesting trends can be observed in the regeneration rate in the region of high air humidity. When the air humidity exceeds 16 g/kg, the regeneration rate for the mixed solution is only slightly greater than that of the LiCl solution, which differs greatly from that in the region of low air humidity, mostly because the mass transfer coefficient decreases as the mass transfer driving force decreases [34, 36]. As the air humidity increases, the mass transfer driving force becomes smaller and smaller. As a result, the mass transfer coefficient also becomes smaller. Because the equivalent absolute humidity content of the 35% LiCl solution (33.2 g/kg) is higher than that of the mixed solution (31.2 g/kg), the mass transfer driving force of the LiCl solution is also greater than that of the mixed solution. As a result, the relative difference in the mass transfer coefficient in the high air humidity region is small, which leads to a small difference in the regeneration rate. However, even though the numerator of the regeneration rate of the mixed solution in the high air humidity region is only slightly greater than that of the LiCl solution, its denominator, which is the difference between the equivalent humidity content and the inlet air humidity, is smaller. The regeneration effectiveness of the mixed solution thus remains much greater than that of the LiCl solution. In line with previous observations, Fig. 13 also shows an improvement in the aspect of both the regeneration rate and effectiveness. The detailed enhancement level varies at various air humidity levels.

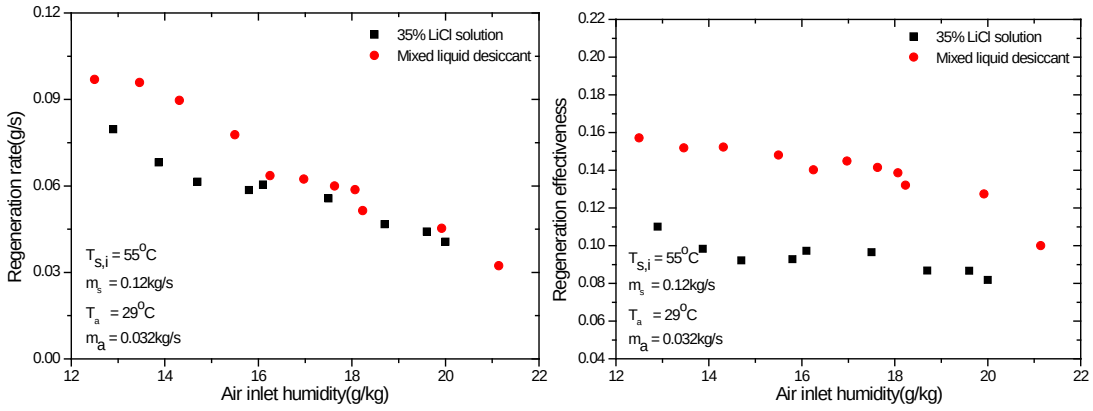

Fig. 13. Influence of air humidity on regeneration.

5.4 Influence of solution flow rate

Fig. 14 illustrates the experimental results on the regeneration characteristics at different solution flow rates. Even though the mass flow rate of the solution has nearly doubled from 0.075 to 0.144 kg/s, the regeneration rate and the effectiveness both remain around a certain value. For the mixed solution, the values are 0.064 g/s and 16.8%, respectively, and for 35% LiCl solution, the values are 0.061 g/s and 15.1%, respectively. On the one hand, when the solution flow rate exceeds the minimum wetting rate [37], the wetting area of the falling film varies little at different flow rates [35]. On the other hand, the mass flow rate of the solution has little effect on the mass transfer driving force during regeneration. Therefore, the change in the solution flow rate causes negligible variation in the regeneration rate and effectiveness. Average relative improvements of 4.7% and 11.3% were obtained for the regeneration rate and the effectiveness with the use of the mixed liquid desiccant compared with the use of the 35% LiCl solution.

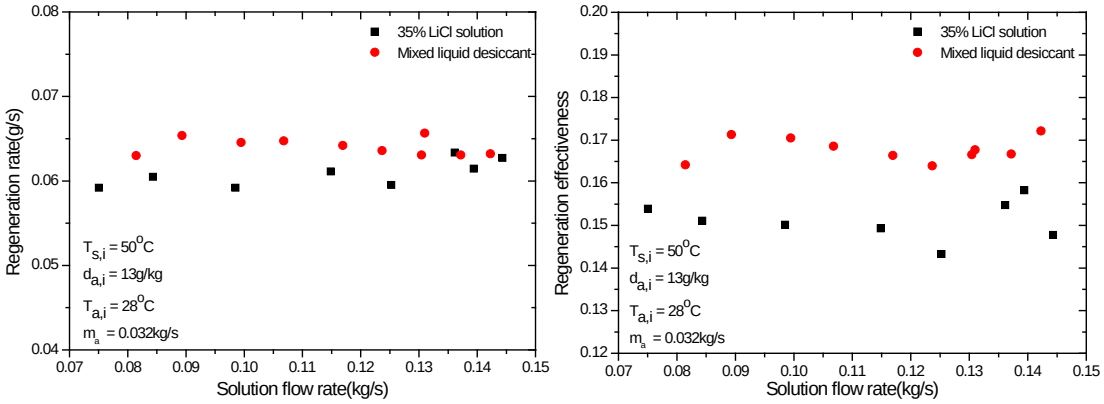

Fig. 14. Influence of solution flow rate on regeneration.

5.5 Influence of solution temperature

Fig. 15 describes and compares the regeneration performance of the mixed and 35% LiCl liquid desiccants at various solution temperatures. It can be seen that the regeneration rate increases from 0.069 to 0.114 g/s for the mixed solution and from 0.064 to 0.104 g/s for the 35% LiCl solution due to an increase in the mass transfer

driving force when the solution temperature is increased from 48°C to 55°C. However, unlike the ascending trend in the regeneration rate, a descending trend is observed for effectiveness. Even though an increase in the solution temperature causes an increase in the absolute humidity change in the numerator of the effectiveness, as shown in Equation 6, the increase in the denominator caused by the increase in the equivalent absolute humidity content is even greater than that in the numerator. As a result, the effectiveness decreases as the solution temperature increases. On average, the relative improvements in the regeneration rate and effectiveness are 8.5% and 19.6%, respectively.

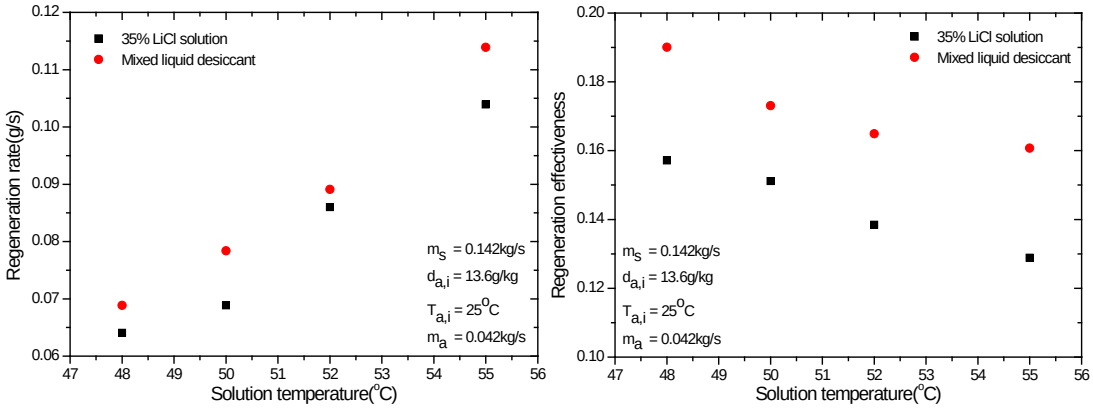

Fig. 15. Influence of solution temperature on regeneration.

5.6 Discussion of the regeneration results

From Figs 11 through 15, it can be concluded that both the regeneration rate and the effectiveness of the newly developed mixed solution show slight improvements over those of the 35% LiCl solution. The values for improvement vary with different operating conditions. Because the vapor pressures of the mixed solution and the 35% LiCl solution are not exactly the same at different temperatures, a comparison of the regeneration rate with different mass transfer driving forces is not convincing. Therefore, only the regeneration effectiveness was compared because it is dimensionless. On average, the relative improvement reaches 14.1% for the mixed solution in various working conditions. The enhancement observed in our study is ascribed to two aspects: an improvement in wettability and a greater fluctuation of the falling film. During the experiments, we observed that the wetting area of the mixed solution differed from that of the 35% LiCl solution. Fig. 16 shows an infrared picture

of falling film on the plate regenerator captured with a high-resolution infrared thermal imager (FLUKE). After postprocessing, the wetting ratio increased from 81.5% for the 35% LiCl solution to 87.8% for the mixed solution, with a relative increase of 7.7%. The increased wetting area makes direct contact with the air and participates in the regeneration process. We continued to cover the mechanism by which regeneration was improved by measuring the contact angles of different solutions. The contact angles of the mixed solution and the 35% LiCl solution were obtained with a standard contact angle goniometer (Rame-hart Instrument Co.) with an accuracy of 0.1° [38], as shown in Fig. 17. The contact angle of the mixed solution was reduced by 8.4° compared with that of that 35% LiCl solution, which is the cause of the improvement in wettability. The film thickness of the solution was measured with a JDC-2008 accumeasure instrument developed by TianJin University with the accuracy of 0.8 μm [4]. The results are presented and compared in Fig. 18. The time average film thickness is defined by Equation 10. The average film thickness of the mixed solution (834 μm) is slightly greater than that of the 35% LiCl solution (671 μm). However, the standard deviation of the film thickness, which is defined by Equation 11, for the mixed solution (31.672 μm) is larger than that of the 35% LiCl solution (25.441 μm). A larger standard deviation of the film thickness means that the fluctuation of the falling film is more significant. The significant turbulence of the falling film not only enhances the heat and mass transfer in the phase interface, it also increases the specific surface area for falling film. As a result, the regeneration performance is enhanced due to the fluctuation on the surface of the falling film.

Not only can the newly developed mixed liquid desiccant significantly reduce the causticity, which will increase the system credibility, it can also enhance the mass transfer performance, which will improve the system efficiency. Although the increase in the mass transfer performance is tiny, the total energy savings will be great in light of the huge amount of energy consumed by heating, ventilation, and air-conditioning systems [7]. Therefore, it is a promising alternative to the conventional LiCl solution for application in a LDCS.

606

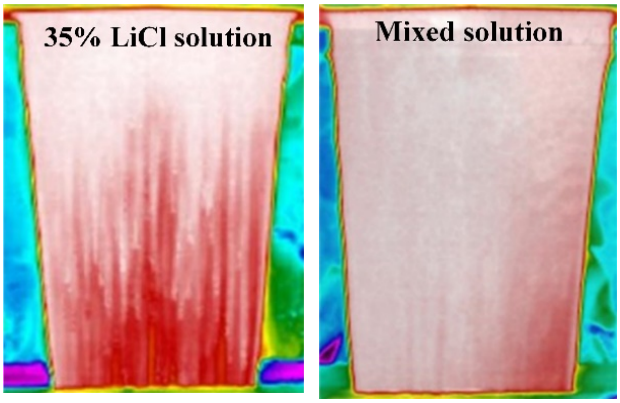

607 Fig. 16. Comparison of wettability on a plate regenerator.

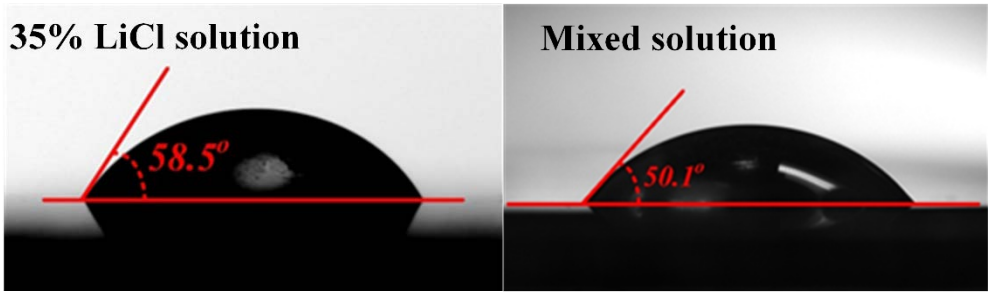

608

609 Fig. 17. Contact angles of the different solutions.

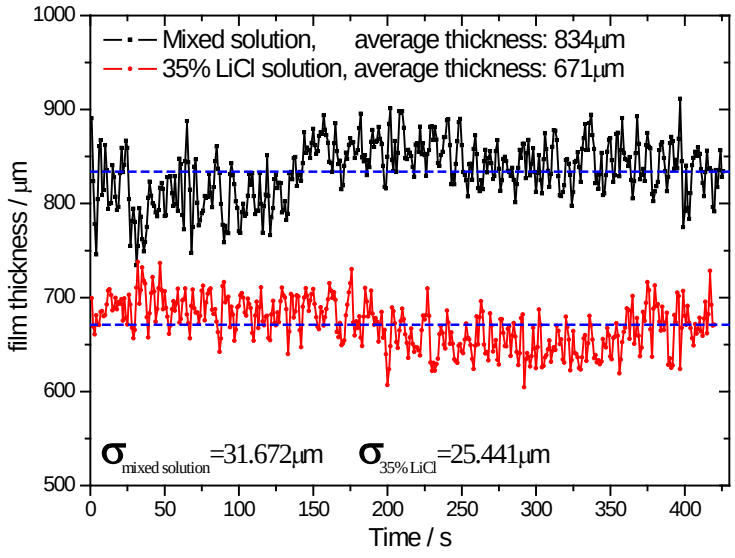

610

611 Fig. 18. Variations in falling film thickness for the different solutions.

612

613 $$\delta_{ave} = \frac{\sum_{t=0}^{T} \delta}{T} \tag{10}$$

614 $$\sigma = \sqrt{\frac{\sum_{t=0}^{T} (\delta - \delta_{ave})}{T}} \tag{11}$$

6 Development of correlation for regeneration effectiveness

This study is the first to develop a mixed liquid desiccant and investigate its regeneration performance under various experimental conditions. To further promote the experimental results and facilitate practical engineering application, a correlation to predict the regeneration effectiveness is proposed based on this study. According to the previous experimental results, the regeneration effectiveness is closely related to the air flow rate, air inlet humidity, and solution temperature. Therefore, it was fitted as the function of the air Reynolds number Re_a, the air inlet humidity $d_{a,in}$, and the solution equivalent humidity d_e. In Equation 12, the influence of the air flow rate and the inlet humidity can be reflected by Re_a and $d_{a,in}$, and the influence of the solution temperature is reflected by d_e. The formula is shown in Equation 12:

$$\eta_{eff} = 0.0184 Re_a^{-0.217} d_{a,in}^{-0.886} (d_e - d_{a,in})^{-0.06} \quad (12)$$

where Re_a is the Reynolds number of air.

Fig. 19 compares the experimental regeneration effectiveness and the effectiveness calculated with the proposed correlation. Almost all of the absolute differences in effectiveness between the experimental and calculated effectiveness are clearly smaller than 10%. For all of the experimental data, the MARD is only 4.01%, which is acceptable for practical application.

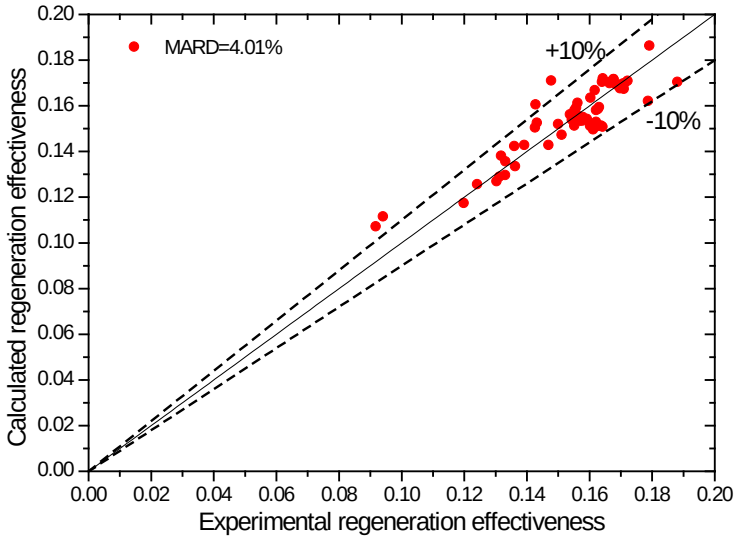

Fig. 19. Comparison between the experimental and calculated regeneration effectiveness.

7 Conclusions

To alleviate the causticity of the LiCl solution, its concentration was reduced by the introduction of hydroxyethyl urea. A new mixed liquid desiccant was developed with the formula of 25% LiCl, 39% hydroxyethyl urea, and 36% water. The vapor pressure, density, dynamic viscosity, and thermal conductivity of the mixed solution were measured at different temperatures. The corrosion behavior of both the mixed solution and the 35% LiCl solution were identified and compared. Finally, the regeneration characteristics of different solutions were also investigated. The main conclusions are as follows:

(1) A new liquid desiccant was successfully developed with the formula of 25% LiCl, 39% hydroxyethyl urea, and 36% water.

(2) The vapor pressure of the new liquid desiccant is nearly the same as that of the 35% LiCl solution between 20°C and 50°C but slightly lower above 50°C. The viscosity of the new mixed solution is much greater than that of the 35% LiCl solution, especially at low solution temperatures, but the differences in terms of density and thermal conductivity are small. Temperature-based polynomials were developed to calculate the thermal properties of the new mixed solution, with a maximum prediction error of 1.38%.

(3) The causticity of the new mixed solution on stainless steel is much less severe than that of the 35% LiCl solution due to its lower concentration of LiCl. The annual corrosion depth decreases from 0.08 mm/Y for the LiCl solution to 0.00267 mm/Y for the mixed solution.

(4) Under the same experimental conditions, the regeneration rate and the effectiveness of the new mixed solution both show slight improvement over those of the 35% LiCl solution. The average relative improvement for regeneration effectiveness is 14.1%, as a result of the increase in the wetting ratio from 81.5% to 87.8% and the significant fluctuation of the falling film on the plate regenerator. The improvement in wettability can be attributed to the decrease in the solution contact angle from 58.5° for the 35% LiCl solution to 50.1° for the new mixed solution.

(5) A correlation was developed to predict the regeneration effectiveness with the given Reynolds number of air and the moisture content of the inlet air for the new mixed

liquid desiccant. The proposed new correlation has a high prediction accuracy, with a MARD of 4.01%, which is reasonable for engineering application.

This study investigated experimentally the thermal properties and regeneration performance of a newly developed mixed liquid desiccant. The new desiccant appears to be a promising alternative for the traditional salt liquid desiccant. The experimental data and empirical correlations in this study can provide meaningful guidance for the design of both regenerators and LDCSs. Moreover, the optimal formula of the mixed liquid desiccant will be refined in our next study to achieve greater system efficiency.

Acknowledgement

The work is financially supported by Hong Kong Research Grant Council through General Research Fund (PolyU 152010/15E) and the Hong Kong Polytechnic University through Central Research Grant (PolyU 152184/17E)..

References

[1] Xiao F, Ge G, Niu X. Control performance of a dedicated outdoor air system adopting liquid desiccant dehumidification. Applied Energy. 2011;88(1):143-9.

[2] Qi R, Lu L. Energy consumption and optimization of internally cooled/heated liquid desiccant air-conditioning system: A case study in Hong Kong. Energy. 2014;73:801-8.

[3] Wan KK, Li DH, Liu D, Lam JC. Future trends of building heating and cooling loads and energy consumption in different climates. Building and Environment. 2011;46(1):223-34.

[4] Luo Y, Wang M, Yang H, Lu L, Peng J. Experimental study of the film thickness in the dehumidifier of a liquid desiccant air conditioning system. Energy. 2015;84:239-46.

[5] Mortazavi M, Isfahani RN, Bigham S, Moghaddam S. Absorption characteristics of falling film LiBr (lithium bromide) solution over a finned structure. Energy. 2015;87:270-8.

[6] Luo Y, Yang H, Lu L. Liquid desiccant dehumidifier: Development of a new performance predication model based on CFD. International Journal of Heat and Mass Transfer. 2014;69:408-16.

[7] Luo Y, Yang H, Lu L, Qi R. A review of the mathematical models for predicting the heat and mass transfer process in the liquid desiccant dehumidifier. Renewable and Sustainable Energy Reviews. 2014;31:587-99.

[8] Dong C, Lu L, Wen T. Experimental study on dehumidification performance enhancement by TiO2 superhydrophilic coating for liquid desiccant plate dehumidifiers. Building and Environment. 2017;124:219-31.

[9] Wen T, Lu L, Dong C, Luo Y. Development and experimental study of a novel plate dehumidifier made of anodized aluminum. Energy. 2018;144:169-77.

[10] Mei L, Dai Y. A technical review on use of liquid-desiccant dehumidification for air-conditioning

application. Renewable and Sustainable Energy Reviews. 2008;12(3):662-89.
[11] Luo Y, Shao S, Xu H, Tian C, Yang H. Experimental and theoretical research of a fin-tube type internally-cooled liquid desiccant dehumidifier. Applied Energy. 2014;133:127-34.
[12] Liu J, Zhang T, Liu X, Jiang J. Experimental analysis of an internally-cooled/heated liquid desiccant dehumidifier/regenerator made of thermally conductive plastic. Energy and Buildings. 2015;99:75-86.
[13] Lee JH, Jung CW, Chang YS, Chung JT, Kang YT. Nu and Sh correlations for LiCl solution and moist air in plate type dehumidifier. International Journal of Heat and Mass Transfer. 2016;100:433-44.
[14] Rafique MM, Gandhidasan P, Bahaidarah HM. Liquid desiccant materials and dehumidifiers–A review. Renewable and Sustainable Energy Reviews. 2016;56:179-95.
[15] Elsarrag E. Dehumidification of air by chemical liquid desiccant in a packed column and its heat and mass transfer effectiveness. HVAC&R Research. 2006;12(1):3-16.
[16] Tsai C-Y, Soriano AN, Li M-H. Vapour pressures, densities, and viscosities of the aqueous solutions containing (triethylene glycol or propylene glycol) and (LiCl or LiBr). The Journal of Chemical Thermodynamics. 2009;41(5):623-31.
[17] Chen L-F, Soriano AN, Li M-H. Vapour pressures and densities of the mixed-solvent desiccants (glycols+ water+ salts). The Journal of Chemical Thermodynamics. 2009;41(6):724-30.
[18] Chen S-Y, Soriano AN, Li M-H. Densities and vapor pressures of mixed-solvent desiccant systems containing {glycol (diethylene, or triethylene, or tetraethylene glycol)+ salt (magnesium chloride)+ water}. The Journal of Chemical Thermodynamics. 2010;42(9):1163-7.
[19] Luo C, Su Q, Mi W. Thermophysical properties and application of LiNO3–H2O working fluid. International Journal of Refrigeration. 2013;36(6):1689-700.
[20] Longo GA, Gasparella A. Experimental analysis on chemical dehumidification of air by liquid desiccant and desiccant regeneration in a packed tower. Journal of solar energy engineering. 2004;126(1):587-91.
[21] Donate M, Rodriguez L, De Lucas A, Rodríguez JF. Thermodynamic evaluation of new absorbent mixtures of lithium bromide and organic salts for absorption refrigeration machines. International journal of refrigeration. 2006;29(1):30-5.
[22] De Lucas A, Donate M, Rodríguez JF. Absorption of water vapor into new working fluids for absorption refrigeration systems. Industrial & engineering chemistry research. 2007;46(1):345-50.
[23] https://pubchem.ncbi.nlm.nih.gov/compound/73984#section=Top.
[24] http://thenakedchemist.com/what-is-urea-and-its-benefits-in-skincare/.
[25] Nitta T, Akimoto T, Matsui A, Katayama T. An apparatus for precise measurement of gas solubility and vapor pressure of mixed solvents. Journal of chemical engineering of Japan. 1983;16(5):352-6.
[26] Lemmon EW, Huber ML, McLinden MO. NIST reference fluid thermodynamic and transport properties–REFPROP. NIST standard reference database. 2002;23:v7.
[27] http://www.corrtest.com.cn/.
[28] Wen T, Lu L, Yang H, Luo Y. Investigation on the Regeneration and Corrosion Characteristics of an Anodized Aluminum Plate Regenerator. Energies. 2018;11(5):1-15.
[29] Roberge PR. Handbook of corrosion engineering: McGraw-Hill, 2000.
[30] Conde MR. Properties of aqueous solutions of lithium and calcium chlorides: formulations for use in air conditioning equipment design. International Journal of Thermal Sciences. 2004;43(4):367-82.
[31] Cengel YA. Fluid mechanics: Tata McGraw-Hill Education, 2010.
[32] Wen T, Lu L, Dong C, Luo Y. Investigation on the regeneration performance of liquid desiccant by adding surfactant PVP-K30. International Journal of Heat and Mass Transfer. 2018;123:445-54.

748 [33] Zhang T, Liu X, Jiang J, Chang X, Jiang Y. Experimental analysis of an internally-cooled liquid desiccant
749 dehumidifier. Building and environment. 2013;63:1-10.
750 [34] Luo Y, Wang M, Yang H, Lu L, Peng J. Experimental study of internally cooled liquid desiccant
751 dehumidification: application in Hong Kong and intensive analysis of influencing factors. Building and
752 Environment. 2015;93:210-20.
753 [35] Wen T, Lu L, Dong C. Enhancing the dehumidification performance of LiCl solution with surfactant
754 PVP-K30. Energy and Buildings. 2018;171:183-95.
755 [36] Yin Y, Zhang X, Wang G, Luo L. Experimental study on a new internally cooled/heated
756 dehumidifier/regenerator of liquid desiccant systems. International Journal of Refrigeration.
757 2008;31(5):857-66.
758 [37] Luo Y. Study on the coupled flow, heat and mass transfer processes in a liquid desiccant
759 dehumidifier: The Hong Kong Polytechnic University, 2014.
760 [38] http://www.ramehart.com/.
761